ACT Publication No. 02-06

Assessment of atmospheric correction methods for Landsat TM data applicable to Amazon basin LBA research

D. Lu, P. Mausel, E. Brondizio, E. Moran

Reprinted from: **International Journal of Remote Sensing. 2002, (23)13: 2651-2671**

Anthropological Center for Training and Research on Global Environmental Change
Indiana University, Student Building 331, 701 E. Kirkwood Ave., 47405-7100, U.S.A.
Phone: (812) 855-6181, Fax: (812) 855-3000, Email: act@indiana.edu, internet: www.indiana.edu/~act

INT. J. REMOTE SENSING, 2002, VOL. 23, NO. 13, 2651–2671

Taylor & Francis
Taylor & Francis Group

Assessment of atmospheric correction methods for Landsat TM data applicable to Amazon basin LBA research

D. LU, P. MAUSEL,

Department of Geography, Geology, and Anthropology, Indiana State University, Terre Haute, Indiana 47809, USA

E. BRONDIZIO and E. MORAN

Anthropological Center for Training and Research on Global, Environmental Change, Indiana University, Bloomington, Indiana 47405, USA

(*Received 26 July 2000; in final form 5 March 2001*)

Abstract. Atmospheric correction is an important preprocessing step required in many remote sensing applications. The authors are engaged in the project 'Human Dimensions of Amazonia: Forest Regeneration and Landscape Structure' in NASA/INPE's Large Scale Biosphere-Atmosphere Experiment in Amazonia (LBA) programme. This project requires use of corrected Landsat TM data since research foci integrate ground-based data and TM to: (1) measure and model biomass; (2) classify multiple stages of secondary succession; (3) model land cover/land use changes; and (4) derive spectral signatures consistent across different study areas. The 30+ scenes of TM data are historic and lack detailed atmospheric data needed by physically-based atmospheric correction models such as 6S (Second Simulation of the Satellite Signal in the Solar Spectrum). Image-based DOS models are based on image measurements and explored in this article for application to LBA study areas. Two methods using theoretical spectral radiance and image acquisition date respectively were used to convert TM DN values to at-satellite radiance. Three image-based models were employed using each method to convert at-satellite radiance to surface reflectance. Analyses of these six different image-based models were conducted. The Improved Image-based DOS was the best technique for correcting atmospheric effects in this LBA research with results similar to those obtained from physically-based approaches.

Nomenclature

λ	wavelength
Gain_λ	radiometric gain
Bias_λ	radiometric bias
DN_λ	Landsat TM digital number
$L_{\lambda sensor}$	apparent at-satellite radiance
$L_{\lambda max}$	maximal spectral radiance at $L_{\lambda range}$ equal to 255
$L_{\lambda min}$	minimal spectral radiance at $L_{\lambda range}$ equal to 0
$L_{\lambda range}$	range of rescaled radiance, 255 for Landsat – 5 TM data
G_λ	calibration gain coefficient
DSL_λ	calibration offset coefficient

International Journal of Remote Sensing
ISSN 0143-1161 print/ISSN 1366-5901 online
http://www.tandf.co.uk/journals
DOI: 10.1080/01431160110109642

MF_λ multiplicative factor for each band
Days number of days since the launch of Landsat – 5 (March 1, 1984)
AF_λ additive constants for each band
R_λ surface reflectance
$L_{\lambda haze}$ path radiance
$Esun_\lambda$ Exo-atmospheric solar irradiance
θ sun zenith angle (or 90 – sun elevation angle)
D distance between Earth and sun (unit: AU)
PI constant, 3.141592
$TAUv$ atmospheric transmittance along the path from the ground surface to the sensor
TAUz is the atmospheric transmittance along the path from the sun to the ground surface

1. Problem

The authors from Indiana University and Indiana State University (IU/ISU) are engaged in the project 'Human Dimensions of Amazonia: Forest Regeneration and Landscape Structure' in NASA/INPE's Large Scale Biosphere-Atmosphere Experiment in Amazonia (LBA) programme. Among the major research foci that integrate ground-based data and Landsat TM data are: (1) measure and model biomass; (2) classify multiple stages of secondary succession; (3) model directions and structure of land cover/land use changes; and (4) derive spectral signatures which are consistent in different study areas. These research themes all require derivation of information from analysis of multitemporal TM data across seven different Amazon study areas. Many of the remote sensing analyses require that TM data from different times and study areas have digital number (DN) values converted into percentage reflectance or in other ways made comparable through atmospheric correction. There is a plethora of methods available, from simple to complex, which address correction and calibration issues (Markham and Baker 1986, Chavez 1988, 1996, Vermote *et al.* 1997). Some of the most accurate methods are physically-based models, which require atmospheric data coincident with remote sensing data acquisition. However, this LBA project uses historic (1985–present) TM data for which atmospheric parameters needed to use physically-based models are unavailable. This is a situation that a majority of scientists faces, whose remotely sensed data were acquired prior to project development. More than 30 TM scenes from seven LBA study areas required the best atmospheric correction possible, excluding physically-based models for which there is too little atmospheric data. The two remaining major categories of corrections are image-based DOS and relative calibration. Based on theoretical considerations, relative calibration is frequently too inaccurate to satisfy LBA research designs, but image-based DOS approaches have proven to be of value even in more sophisticated research designs. There are many variations of image-based models and this research explores six of the most promising variations to find the best approach to atmospherically correct the large TM data library used in the multi-year IU/ISU LBA research. The exploration of these six models as applied in the Altamira, Brazil study area should provide insights to other scientists facing problems similar to that found in LBA research. The methods, theory and characteristics of the six image-based approaches are provided using an actual case study and the results can be matched to project needs of others to identify the most

appropriate correction methods for a given atmospheric correction problem. In this research two of the six image-based approaches best addressed LBA problems for reasons that are thoroughly explored in other sections of this article.

2. Reasons for radiometric and atmospheric correction

Analysis using uncorrected data assumes that the radiance of vegetation, soil, water and other objects of interest have sufficiently different reflectance characteristics for differentiation and that atmospheric effects are not sufficiently great to affect their basic spectral separations. However, with extensive and intensive applications of remotely sensed data in a variety of applications important in LBA research, atmospheric effects become very important. There are at least six reasons in support of radiometric and atmospheric correction for Landsat TM or other remotely sensed data: (1) multi-temporal TM data applications such as in land use/cover change detection; (2) across scene (across path) comparison of spectral information of land cover types; (3) multi-sensor data applications such as multiple image mosaic to spatially produce a large image, multi-sensor data integration such as TM and SPOT images; (4) quantitative analysis by combining field survey data with spectral data for applications such as biomass estimation; (5) selected special applications such as using visible TM bands for mapping shoals and aquatic plants beds; and (6) band ratio operations such as vegetation indexes.

3. Study area and data characteristics

The study area is located near Altamira, Brazil (TM path and row: 226 and 62) and is one of seven project study areas (figure 1). This region has been subject to colonization, which focused on small and large-scale agricultural activities since 1970. Land cover comprised dense and liana forests, various stages of secondary vegetation, dense and sparse pasture, with some crops and agroforestry. Field studies relevant to current LBA research began in 1971 and have continued to the present. This long-term fieldwork has resulted in providing the authors with one of the largest ethnographic, social-economic, land use/land cover, vegetation and soil inventory databases in the Amazon. Therefore, the study area presents an ideal laboratory to study land cover trajectories and biomass dynamics representative of the eastern Amazon (Moran 1981, Mausel *et al.* 1993, Brondizio *et al.* 2000). The image acquisition date, sun elevation angle and image characteristics used in this study are listed in table 1. The 1985 image is cloud free, the 1987 and 1988 images have some cloud cover and the 1991 image has heavy haze with striping on the first two TM bands. This variety of data quality is representative of many research situations in the region.

4. Atmospheric correction background and methods

Atmospheric conditions can vary significantly both spatially and temporally as a result of molecular scattering and absorption. The atmosphere has selective scattering characteristics; that is, different wavelengths have various atmospheric influences on TM images. There are two main effects of atmosphere, i.e. scattering and absorption. The effects of them depend on the wavelength of a given sensor system. The main effects of the atmospheric scattering on remotely sensed data are upwelling atmospheric radiance or path radiance (Slate 1980) and atmospheric absorption with multiplicative characteristics. Generally, in infrared TM bands, the main effects of the atmosphere are from air molecule and aerosol particle scattering, which are

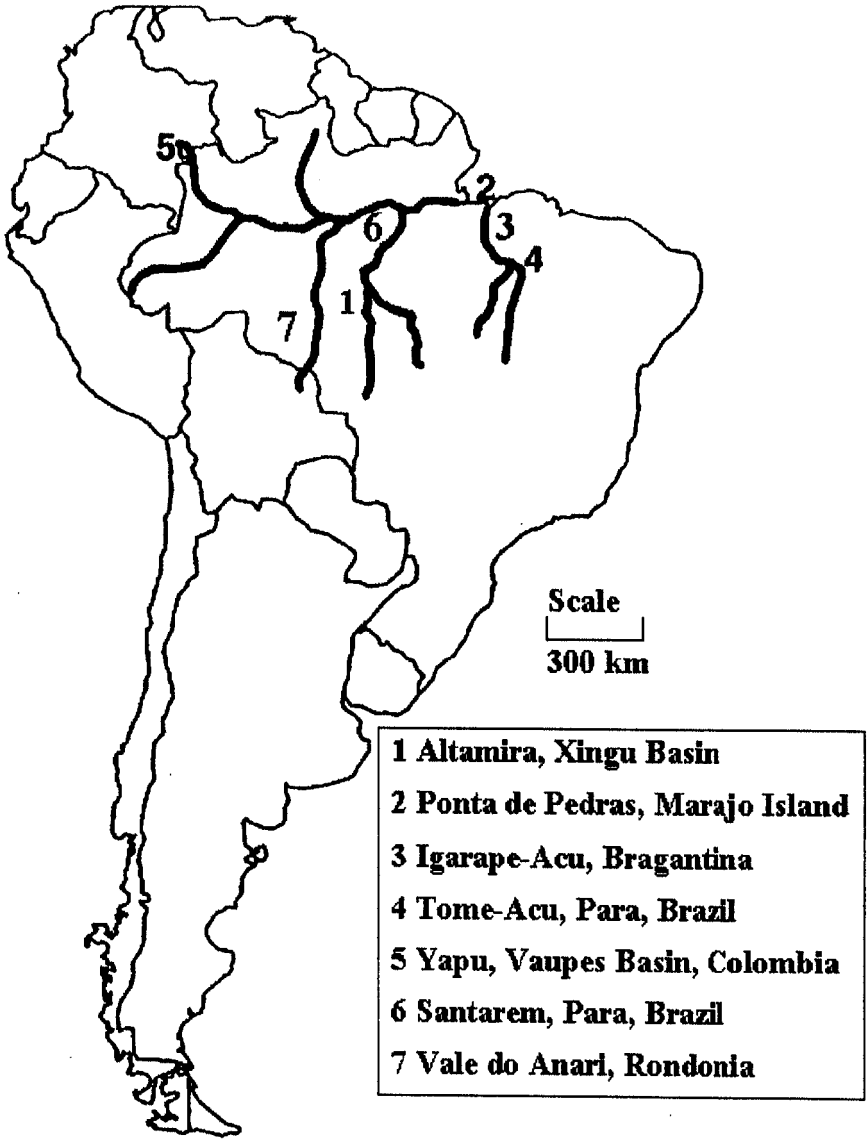

Figure 1. The seven study areas of the IU/ISU/INPE research program. Altamira (site 1) is the specific area used in this article.

Table 1. Characteristics of Landsat TM images used in Altamira research.

Images acquisition date	Sun elevation angle (°)	Cloudy conditions (%)
4 August 1985	48	Cloud free: 0%
23 June 1987	45	Cloudy: 10%
11 July 1988	46	Cloudy: 10%
20 July 1991	45	Cloud free: 0%

additive and create image haze. Air molecules are stable and obey Rayleigh's scattering rule, but the character of aerosol particles is often variable and their influence is difficult to estimate. In visible bands, the absorption caused by water vapor or other gases is very weak and can be ignored, thus the impact of short wavelengths is mainly from Rayleigh scattering. However, in near infrared and middle infrared wavelengths, the influence of air molecules and aerosol particle scattering can be negligible, the main impact is from the atmospheric absorption caused by water vapor, carbon dioxide, methane and other gases. Normally, the contents of carbon dioxide, carbon oxide and methane are stable, but water vapor is variable. A good model should have the capability to simulate the above phenomena and to correct the influences caused by scattering and absorption.

Two different groups of calibration methods can be identified, that is, the absolute radiometric correction and relative calibration method (Thome *et al.* 1997). The absolute correction method converts remotely sensed digital numbers into surface reflectance or radiance by removing the effects caused by atmospheric attenuation, topographic condition and other parameters. It is necessary to focus on the extraction of subtle differences in reflectance to estimate biophysical properties such as biomass and forest volume, when establishing relationships between ground truth data and remotely sensed measurements. The extension of spectral signatures of features of interest over space and time is vital for many types of research. Common models for absolute atmospheric correction include 6S (Second Simulation of the Satellite Signal in the Solar Spectrum), MODTRAN (Moderate Resolution Atmospheric Radiance and Transmittance Model), LOWTRAN, image-based DOS (dark object subtraction) models, etc. A second class of calibration method focuses on relative atmospheric correction. It is used to remove or normalize the variation within a scene and normalize the intensities between images of same study area collected on different dates. The methods for relative correction can be histogram adjustment, dark-pixel subtraction, and multi-date normalization using a regression model approach.

According to the model characteristics and complexity, three types of models can be grouped. The first type of models is physically-based, which require many simulation submodels that use many parameters. Such models can produce high surface reflectance accuracy. These models include 6S, LOWTRAN, and MODTRAN which are often very complex and require many input parameters from the *in situ* field atmospheric information acquired at the time of remote sensing data acquisition. A second class of models is image-based DOS which assume that the atmospheric impact is uniform on the whole study area and that dark objects exist. Such models do not require any *in situ* atmospheric information. Inputs required to implement these models are mainly based on image measurements and the remote sensing data header file, which provides some important information such as image acquisition date, sun elevation angle, gain and bias. When an image header file is not available then the image acquistion date can be used to derive needed parameters. The third method focuses on relative calibration and develops models based on histogram matching, dark pixel subtraction or regression equations.

4.1. *Physically-based calibration models*

Physically-based models are the most complex and highly accurate models used for converting digital numbers into surface reflectance. For example, in the 5S model the input parameters involve the geometric conditions such as the sun zenith angle

and azimuth angle, the atmospheric components such as water vapor, carbon dioxide, ozone, and oxygen, the pressure and temperature profile, the aerosol type and concentration, the spectral bands of observation and the ground reflectance type and spectral variation (Tanre *et al.* 1990). The 6S code adds some new absorbing gases such as methane, nitrous oxide, and carbon monoxide and also considers Rayleigh and aerosol scattering and gas absorption between 0.25 and 4.00 μm at a spectral resolution of 2.50 nm. This 6S version permits calculations of near-nadir aircraft observations, accounting for target elevation and non-lambertian surface conditions. More accurate and complex algorithms for calculating Rayleigh and aerosol scattering, gaseous absorption and transmission were adopted. The coupling between the BRDF (Bi-directional Reflectance Distribution Function) and the downward radiance at the surface level was included (Vermote *et al.* 1997). The MODTRAN model includes all the functional capabilities of LOWTRAN7 but uses a more accurate and high resolution molecular band model with 2 cm^{-1} resolution (20 cm^{-1} resolution of LOWTRAN7). The MODTRAN model uses a stored spectral data base for H_2O, CO_2, O_3, N_2O, CO, CH_4, O_2, NO, SO_2, NO_2, NH_3 and HNO_3. This model includes the effects of scattering (such as Rayleigh and Mie) and allows user specification for profiles of temperature, water vapor density, ozone, aerosols and any other gases which may vary with time (Richter 1985, 1996b, Palluconi *et al.* 1996). Putsay (1992) developed a simplified method to partly eliminate the blurring effects of the atmosphere using the incidence and observation direction, the optical parameters of the atmosphere, the single scattering albedo and the angular scattering phase function for the molecular and aerosol mixture for the four spectral bands. Rahman and Dedieu (1994) used a semi-empirical formulation to describe the different interactions of solar radiation with atmospheric constituents during its traverse through the atmosphere. The physically-based models can be used in different atmospheric conditions including seasonal and geographic variations, atmospheric scattering, and absorption and can provide highly accurate surface reflectance of varying wavelengths.

4.2. *Image-based calibration models*

Physically-based models require *in situ* atmospheric measurements and radiative transfer codes to correct for atmospheric effects. In practice such models have a main disadvantage in that it is often impossible to collect the *in situ* atmospheric parameters for many applications, especially when using historical remotely sensed data. Hence, it is necessary to develop a model that purely depends on digital image information that does not require gathering of *in situ* field measurements during the satellite overflight. Different levels of image-based models have been developed. The most straightforward method is the apparent reflectance model (Markham and Barker 1985, 1986, 1987, Price 1987, Hall *et al.* 1988, 1989, Chavez 1989, Hill 1991), which converts apparent or at-satellite reflectance to surface reflectance by correcting sensor gain, offset, solar irradiance and solar zenith angle, but ignoring the correction of atmospheric scattering and absorption. Dark object subtraction (DOS) models take path radiance into consideration in addition to the function of the apparent reflectance model. It assumes that the multiplicative effect from atmosphere is constant, the surface is Lambertian, the path radiance is uniform and some pixels within the image are in complete deep shadow and their radiance captured by satellite sensor are due to the atmospheric scattering (path radiance). The DOS model (Chavez 1988, 1989, Fraser *et al.* 1992, Moran *et al.* 1992, Milton 1994) was used to

remove the additive scattering component caused by path radiance based on the assumption that an absolute dark object exists within the image. The atmospheric effects are wavelength dependent, including atmospheric scattering and absorption that have additive and multiplicative effects on the image. Therefore, the Improved Image-based DOS model (Teillet 1986, Richards 1993, Olsson 1995, Chavez 1996, Jensen 1996, Richter 1997) includes the correction of atmospheric transmittance through optical thickness values at a given wavelength or using the default transmittance values derived from the *in situ* atmospheric. Gilabert *et al.* (1994) used an inversion technique based on a simplified radiance transfer model, assuming the presence of a dark object and using a combination of TM 1 and TM 3. The actual aerosol model is estimated through the wavelength dependence of the aerosol path radiance. In the improved image-based model, the key problem is how to estimate the aerosol optical thickness and how to identify the path radiance value (haze). There are at least three methods to obtain optical thickness. Method 1 uses ground-based values of the measurements of solar transmission. Radiative transfer codes and *in situ* field measurements have been used to estimate the optical thickness (Moran *et al.* 1992, Leprieur *et al.* 1995, Chavez 1996, Richter 1996a, b). Method 2 uses the data from remote sensing measurement itself. For instance, dense dark vegetation in the visible spectrum, water in the red and near infrared spectrum and a scattering phase function, was used to derive the atmospheric optical thickness (Kaufman and Sendra 1988, Fraser *et al.* 1992). Method 3 uses simulations from climate data. Path radiance can be determined from the dark pixels of the image such as cloud shadows, topographic effects, clear water bodies, dense vegetation such as coniferous forest with very low reflectance in the blue and red region (TM 1 and TM 3) (Chavez 1989, Hill 1991, Gilabert *et al.* 1994).

4.3. *Relative calibration methods*

Histogram adjustment of a single image method is based on the assumption that near-infrared and middle infrared image data are free of atmospheric scattering effects, while the visible image data is strongly influenced by the atmospheric effects, especially in visible wavelength image data such as Landsat TM 1. This method attempts to find the desired value separately in the visible bands for atmospheric correction. Different methods can be used to identify the value, for instance, by evaluating the histogram of brightness values, evaluating the values of very dark objects such as deep and clear waters, minimum value of the image data and simple linear regression. Dark pixel subtraction is often used. It assumes that the pixel of lowest DN in each band should be zero and hence its radiometric value (DN) is the result of atmosphere induced additive errors (ERDAS Inc. 1997). After the desired value of atmospheric scattering is identified for each visible band, the algorithm for correcting atmospheric effects can be defined as output brightness value for a given band equal to the difference between original brightness value and the atmospheric scattering value. That is, output DN = input DN – scattering value of the dark object (Jensen 1996).

Multiple-date image normalization uses histogram matching and regression modelling to normalize one date of image into another so that the multiple dates of images have approximately the same radiometric characteristics. When the atmospheric conditions are unknown, pseudo-invariant ground targets may be used to normalize multi-temporal data sets to a single reference scene. Multiple dates of remotely sensed data are required in land use/cover change detection. Multiple image

data are usually not captured on anniversary dates, thus sun angle, atmospheric conditions and soil moisture likely vary from date to date. Normalization can be used for minimizing the effects caused by the differences in sun angle, atmospheric conditions and soil conditions. Regression models are usually used for image normalization in multi-date image processing (Volchok and Schott 1986, Schott *et al.* 1988, Hall *et al.* 1991, Muller 1993). One date of image acts as the reference image and another date of image as the predicted image. The regression equation is developed by correlating the values of the normalization targets in both the image being normalized and the reference image, based on the assumption that the values of the normalization targets are constant and any changes of these values in other images are caused by the satellite sensor, atmospheric conditions and soil conditions. This relationship can be described as: $DNy = a + b$ *DNx, where the regression coefficient b is a multiplicative component, which can correct for the difference in sun angle, atmosphere, etc. The intercept a is an additive component, which can correct for the difference in atmospheric path radiance between dates of image data. The key step in establishing the regression relationship is to obtain the a and b parameters. This can be derived from a set of sample data selected from the invariant objects such as an undisturbed dense mature forest, bare soil or a road in both dates of images based on the assumption of similar environmental conditions. Olsson (1993) concluded that multiple regression function from all TM bands were considerably better than the band-to-band regression, especially for bands TM 1 through TM 3.

5. Topographic correction

The above mentioned atmospheric correction models are based on the assumption that the surface is a flat horizon surface with cloud free atmosphere. The topography is not considered. In rugged terrain, special emphasis should be put on the influence of topography on solar irradiance and on atmospheric effects. In general, the irradiance components and atmospheric parameters are first corrected for the horizontal surface using physically-based models or image-based DOS models, then the influences of topography on the parameters are integrated and adjusted using DEM data (Teillet *et al.* 1982, Teillet 1986, Kawata *et al.* 1988, Leprieur *et al.* 1988, Proy *et al.* 1989, Duguay and Ledrew 1992, Itten *et al.* 1992, 1993, Meyer *et al.* 1993, Kusaja and Kawata 1994, Stefan and Itten 1997). Teillet *et al.* (1982) described four topographic slope-aspect correction methods, which are statistical-empirical, simple cosine and two semi-empirical methods (the Minnaert method and the C-correction). These methods can be used in rugged or mountainous regions for correcting the effects caused by topography. Meyer *et al.* (1993) employed the above four correction methods for the reduction of slope-aspect effects in a Landsat TM data set in a mountainous test site to analyse the influence on forest classification and on the visual appearance of the image. They concluded that the statistical empirical, Minnaert and C-correction approaches yield an improvement of the forest classification and an impressive reduction of the visual topography effect.

6. Overview of atmospheric correction methods

Much research has been conducted during the past 30 years in atmospheric correction of Landsat TM data and other spectral data. Previous studies have confirmed that atmospheric correction can improve results in a variety of TM data. Physically-based calibrated models such as 6S and MODTRAN can convert remotely sensed digital data to absolute surface reflectance with high calibration accuracy if the

atmospheric information at the time of satellite overflight is available. These types of models are based on complex algorithms that require collecting *in situ* atmospheric information or simulation data. However, in practice, the atmospheric conditions are variable and are often difficult to collect, especially for older remotely sensed data. This disadvantage greatly limited their applications in atmospheric corrections. Image-based calibration models, such as the Improved Image-based DOS model, avoid collecting *in situ* atmospheric information. They purely depend on the intrinsic image information such as gain, offset, sun zenith angle, path radiance and atmospheric transmittance. However, much attention should be paid to identifying path radinace and transmittance. The Improved Image-based DOS model can convert DN values to the surface reflectance with high accuracy (Chavez 1996). The relative calibration method is also used for normalizing DN values among multi-temporal images for change detection application. The disadvantage is that this method can not remove the atmospheric impacts because they are different in various wavelengths. Thus the relative calibrated data are not suitable for quantitative analysis such as image ratio and estimation of biomass by combination of ground survey data.

7. Atmospheric correction methods used in LBA research

The factors that influence Landsat TM DN values have many possible causes including: (1) satellite instrumentation; (2) differences in illumination associated with seasonal change; (3) atmospheric conditions when the image data were captured; and (4) terrain factors such as elevation, aspect and slope that influence the solar irradiance and water vapor distribution. For LBA Amazon research, atmospheric correction is the most important preprocessing factor and also is the most difficult to correct due to the complexity of atmospheric conditions in time and space. The atmospheric impact on reflectance is wavelength dependent. For example, the main sources of spectral scattering in a visible wavelength are from air molecules and aerosol particles scattering, while in near infrared and middle infrared wavelength, the water vapor, carbon dioxide and other gas absorption are the main absorptive factors.

The objective of atmospheric correction is to convert remotely sensed DN to ground surface reflectance. Many models have been developed for the atmospheric correction. Different models have different requirements for the input parameters. Which model is used depends on the requirements of a research project and what information is available for atmospheric correction. In the Amazon Basin research, historical Landsat images are the most important data sets used to analyse deforestation and land use changes. For these images, *in situ* measurements of atmospheric parameters are impossible to obtain and even the header files of some images are not readily available. Sometimes the only available information is the image acquisition date. In such a situation, physically-based models such as 6S can not be employed for correction. However, these remotely sensed images can be used for the biomass estimation and forest characteristic analysis by incorporating field survey data. This approach requires the remotely sensed digital numbers to be converted to surface reflectance with reasonable accuracy. The Improved Image-based DOS model, DOS model and Apparent Reflectance model were tested for their suitability to address LBA project research needs.

The first step of the image-based atmospheric correction method is to convert remotely sensed DN values to at-satellite radiance based on the gain and bias for each band, which was provided from image header file, that is:

$$L_{\lambda sensor} = \mathrm{Gain}_{\lambda} * \mathrm{DN}_{\lambda} + \mathrm{Bias}_{\lambda} \quad (1)$$

However, for most historical Landsat images of the Altamira area in this research, the gain and bias for each band are not available. The only available information that can be obtained is the image acquisition date. Two methods for converting TM DN values to at-satellite radiance were employed in this research. The first method is based on maximal and minimal spectral radiance value for each band, which was provided by Markham and Barker (1986).

$$L_{\lambda sensor} = (L_{\lambda max} - L_{\lambda min})/L_{\lambda range} * \mathrm{DN}_{\lambda} + L_{\lambda min} \quad (2)$$

The second method is based on the image acquisition date (Thome *et al.* 1994, Teillet and Fedosejevs 1995).

$$L_{\lambda sensor} = (\mathrm{DN}_{\lambda} - DSL_{\lambda})/G_{\lambda} \quad (3)$$

$$G_{\lambda} = MF_{\lambda} * \mathrm{Days} + AF_{\lambda} \quad (4)$$

The first step is to eliminate or reduce the effects resulting from the satellite sensor system, then the next step is to convert the apparent at-satellite radiance to surface reflectance which involves the correction of effects caused by both solar angle and the atmosphere. The earth-sun distance can be obtained from the Astronomical Almanac according to the image acquisition date. The sun zenith angle can be obtained from at least two sources. One is from the image header file if available. The alternative is to calculate the sun zenith angle from the mathematical calculation based on the image acquisition date and time and the longitude and latitude of the study area (Campbel and Norman 1998). Several techniques have been developed for the atmospheric correction based on the assumptions of: cloud free images, Lambertian surface and uniform path radiance. The path radiance caused by atmospheric molecules and aerosols can be corrected by dark-object subtraction (Chavez 1989, Teillet and Fedosejevs 1995) or through the radiative transfer code (Moran *et al.* 1992). The atmospheric transmittance caused by atmospheric absorption can be estimated from the optical thickness (Chavez 1996) or using *in situ* field atmospheric measurement. Three techniques based on the image information were used in this research. The first method is the Apparent Reflectance model. It corrects the effects caused by the solar radiance and sun zenith angle, ignoring the effects caused by atmospheric scattering and absorption. This method is very simple and easy to apply because it does not need any *in situ* field measurements.

$$R_{\lambda} = \mathrm{PI} * D^2 * L_{\lambda sensor}/(Esun_{\lambda} * \mathrm{COS}(\theta)) \quad (5)$$

The second method is called the DOS model (dark-object subtraction). This method is also strictly an image-based procedure. It corrects for the effects caused by sun zenith angle, solar radiance and atmospheric scattering, but can not correct the atmospheric absorption.

$$R_{\lambda} = \mathrm{PI} * D^2 * (L_{\lambda sensor} - L_{\lambda haze})/(Esun_{\lambda} * \mathrm{COS}(\theta)) \quad (6)$$

The third method is the Improved Image-based DOS model. It not only has all the functions of the above two models but also takes the atmospheric multiplicative transmittance components into account.

$$R_{\lambda} = \mathrm{PI} * D^2 * (L_{\lambda sensor} - L_{\lambda haze})/(\mathrm{TAUv} * Esun_{\lambda} * \mathrm{COS}(\theta) * \mathrm{TAUz}) \quad (7)$$

The TAUv and TAUz can be estimated from optical thickness. Chavez (1996) found two approximate methods to estimate the atmospheric transmittance. One is using the cosine of the solar zenith angle for TAUz and entitled the COST model,

another method is using default TAUz values which are the average for each spectral band derived from rediative transfer code. The TAUv is equal to 1 because the viewing angle for Landsat TM images is zero. Table 2 lists the constants that were used in these models.

Different calibration methods based on image information are described above, but which method is most suitable for atmospheric correction in the Amazon basin area? Two evaluation methods can be employed. Comparison of spectral graphs of the same land cover, derived from different calibration models, can be used to analyse which calibration method is the most reasonable according to the spectral distribution in different wavelengths. The spectral graph of invariant land cover from multitemporal imageries, derived from the same calibration method, can be used to analyse the reliability of this method. This is true because reflectance of the same land cover should have the same value on the different image acquisition dates if atmospheric and radiometric effects are removed and environmental conditions are similar. Statistical analysis of the reflectance derived from different calibration models can be used to analyse how much the image information is maintained after calibration. For example, more information is contained in an image that has a higher standard deviation and wider range of reflectance mean.

8. Results and discussion

In this article two methods were used to convert Landsat TM DN values to at-satellite radiance, that is, using the experimental maximal and minimal spectral radiance equation (2) and using the image acquisition date equations (3) and (4). Three methods were used for converting at-satellite radiance to surface reflectance. They are the apparent reflectance model in equation (5), the DOS model in equation (6), and the Improved Image-based DOS model in equation (7). These methods are summarized in table 3.

8.1. *Spectral analysis of surface reflectance*

Figure 2 shows the comparison of forest reflectance resulting from different calibration methods. The reflectance of each band is the average value sampled from the dense mature forests at different sites. It is assumed that dense mature forests have a stable surface reflectance at the spatial and temporal scales. The apparent reflectance

Table 2. Constants used in equations (2) to (7).

TM band	$L_{\lambda max}$	$L_{\lambda min}$	MF_λ	AF_λ	DSL_λ	$Esun_\lambda$	TAU_Z
TM 1	15.21	−0.150	−0.0000358	1.376	2.523	195.29	0.70
TM 2	29.68	−0.280	−0.0000210	0.737	2.417	182.74	0.78
TM 3	20.43	−0.120	−0.0000104	0.932	1.452	155.00	0.85
TM 4	20.62	−0.150	−0.0000032	1.075	1.854	104.08	0.91
TM 5	2.719	−0.037	−0.0000264	7.329	3.423	22.075	**
TM 7	1.438	−0.015	−0.0003810	16.020	2.633	7.496	**

Notes: 1. $L_{\lambda max}$, $L_{\lambda min}$ and $Esun_\lambda$ are cited from Mark and Bark (1986).
2. MF_λ, AF_λ and DSL_λ are cited from:
http://www.ccrs.nrcan.gc.ca/ccrc/tekrd/rd/ana/calval/landst5e.html.
3. TAU_Z are cited from Chavez (1996).
4. ** uses the default values (1.0) due to lack of the values in the Chavez (1996) paper.

Table 3. Methods used for atmospheric correction of TM scenes in the Amazon Basin.

Methods used to converting at-satellite radiance to surface reflectance	Methods used to converting DN to at-satellite radiance	
	Date method	Maximal & minimal radiance
Apparent reflectance model	DATE1	GAIN1
Dark object model (DOS)	DATE2	GAIN2
Improved image based DOS model	COST1	COST2

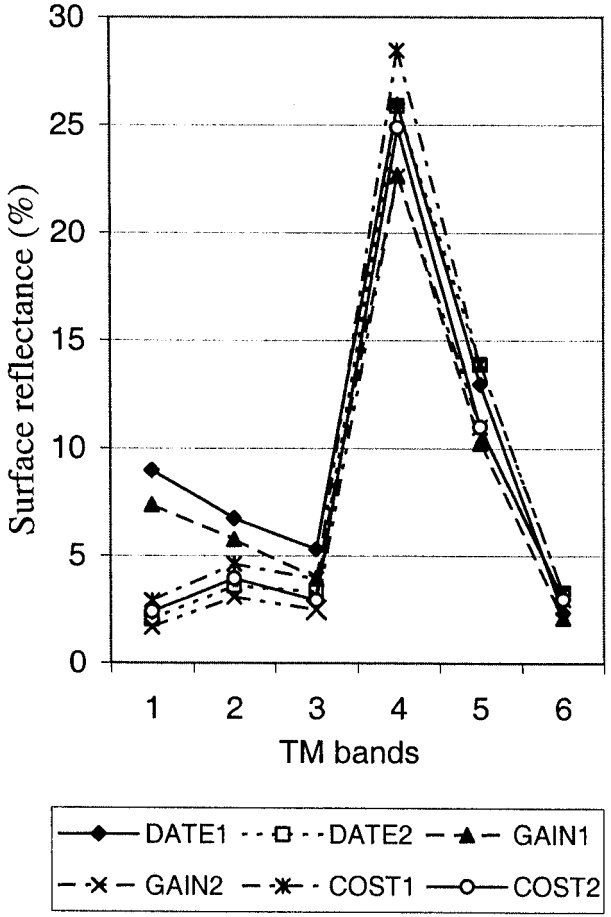

Figure 2. Comparison of calibration methods (forest).

model (DATE1 and GAIN1) resulted in high surface reflectance in the visible bands, i.e. TM 1,TM 2 and TM 3. This is because the apparent reflectance model only corrects for the effects caused by the sun angle, sun-earth distance and the solar radiance. It ignores the effects of atmospheric scattering. The visible bands are mainly influenced by the atmospheric scattering, which provided image additive effects. The DOS model (DATE2 and GAIN2) corrects for the sun angle, sun-earth distance, solar radiance and the atmospheric scattering. The forest reflectance in the visible bands is very low, especially in TM band 1 and TM band 3 due to the strong

chlorophyll absorption. The green band (TM 2) has a lower reflectance peak because of the high chlorophyll reflectance of forest leaves. The Improved Image-based DOS model (COST1 and COST2) has higher reflectance values than those obtained from the DOS model and the apparent reflectance model. In addition, the reflectance from COST1 has higher values than that from the COST2 due to the different method used in converting Landsat DN values to the at-satellite radiance. In the near and middle infrared bands the COST method has higher reflectance than that from any other methods used in this research because it reduces the effects caused by the atmospheric transmittance which decrease the surface reflectance. The DOS model and apparent reflectance model produced very similar results in the near and middle infrared bands because atmospheric scattering is very weak in these wavelengths. If the atmospheric scattering is ignored, the two models became the same. Using the image acquisition date in the first conversion step, higher surface reflectance was found than when using the experimental maximal and minimal spectral radiance. Figure 3 shows the surface reflectance of bare soils, an average from the sampled sites based on the assumption that the bare soils of the same soil type have the similar reflectance among different sites. This figure further confirms that using the image acquisition date in converting Landsat TM DN values to at-satellite radiance can

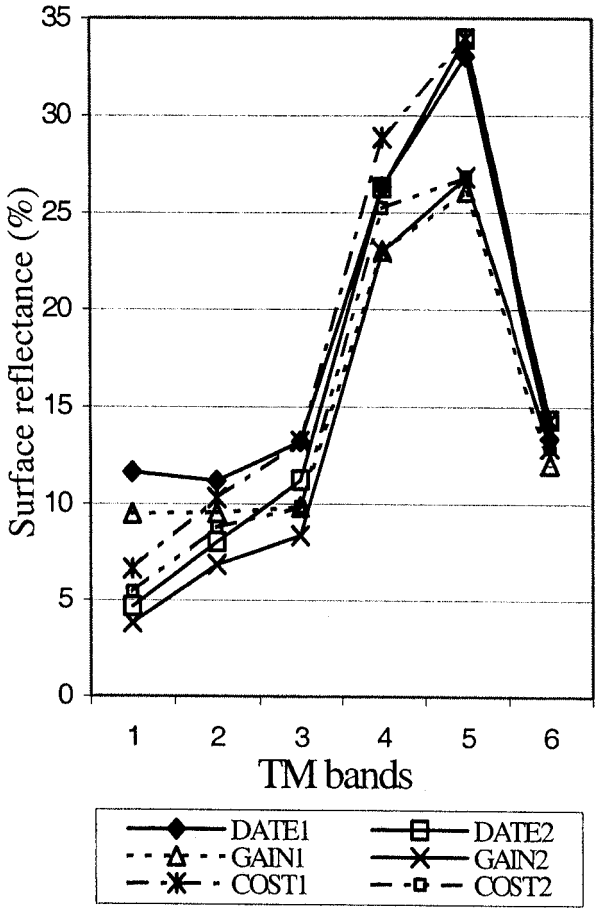

Figure 3. Comparison of calibration methods (soil).

produce higher reflectance in the final results than that using the maximal and minimal radiance. The method of using maximal and minimal radiance underestimated the surface reflectance, especially in the near and middle infrared wavelengths. The Improved Image-based DOS model can produce higher reflectance due to its capability of correcting for the atmospheric scattering and transmittance. The COST1 method provides the most reasonable results for the Altamira research. Figure 4 shows the comparison of mature forest reflectance produced from the COST1 method that was used in the atmospheric correction of multiple dates of TM images. This method provides stable and good results in these four dates of TM images. The 1991 image has a relative high surface reflectance comparing the other three images, especially in the visible wavelengths. Analysing the 1991 image through visually checking the raw images and their statistics indicates that heavy haze exists and the visible bands have striping problems. The graph also indicates that the path radiance can not be ignored in the near infrared and middle infrared wavelength when heavy haze exists. The clouds and shadows also have some impacts in correcting for the atmospheric effects due to the fact that there is more humidity in the atmosphere during cloudy weather compared with clear weather. The high humidity resulted in lowering surface reflectance, especially in the near and middle infrared wavelengths.

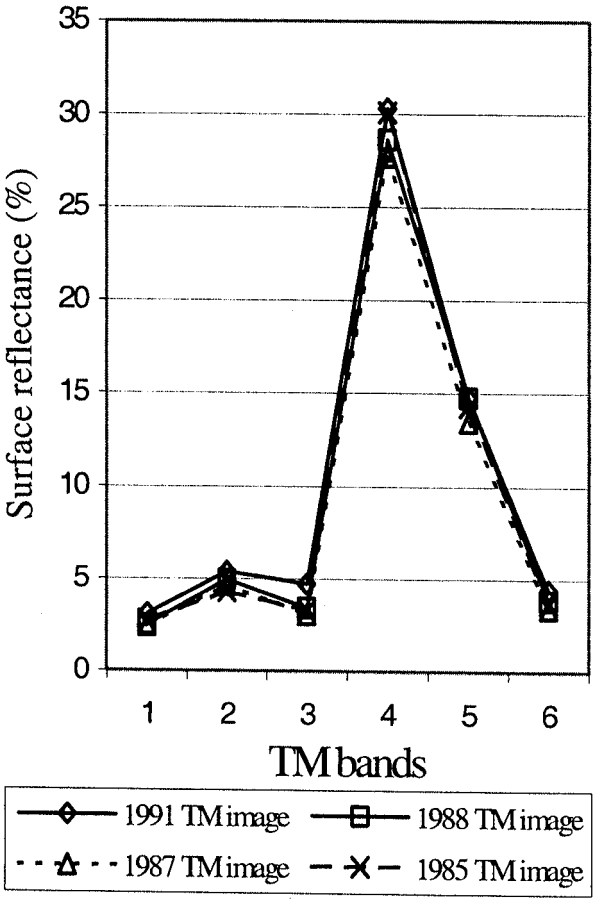

Figure 4. Comparison of multidate images—forest (COST1 Method).

Figure 4 shows that after calibrating using the COST1 method, all four dates have nearly identical spectral characteristics for mature forests. This result provides high quality multitemporal analysis. Figure 5 shows the dense mature forest DN values of the raw TM data sets of different dates. It is evident that the 1991 image has higher DN values in the visible bands than that of the other three dates of images, but has relative lower DN values in the near and middle infrared bands comparing with the 1985 image with clear weather. This also confirmed that the heavy haze increases the reflectance in visible bands and reduces the reflectance in the near and middle infrared bands. This is because the haze has additive function that makes the DN values higher than that of clear weather in the short wavelength, but with the increase of wavelength, the haze effect can be very weak, especially in the TM 7 band. Clouds also influence the reflectance, especially in the near and middle infrared wavelengths that have decreased reflectance due to the atmospheric absorption. Landsat TM 4 and TM 5 bands are seriously affected by the clouds when compared with the cloud free images. Figure 6 compares 1991 TM spectral responses of mature forest and secondary succession features between raw and calibrated images after stripping effects were removed. The quality of calibrated imagery was greatly improved, especially in visual bands, after removing the stripping effects for atmospheric correction.

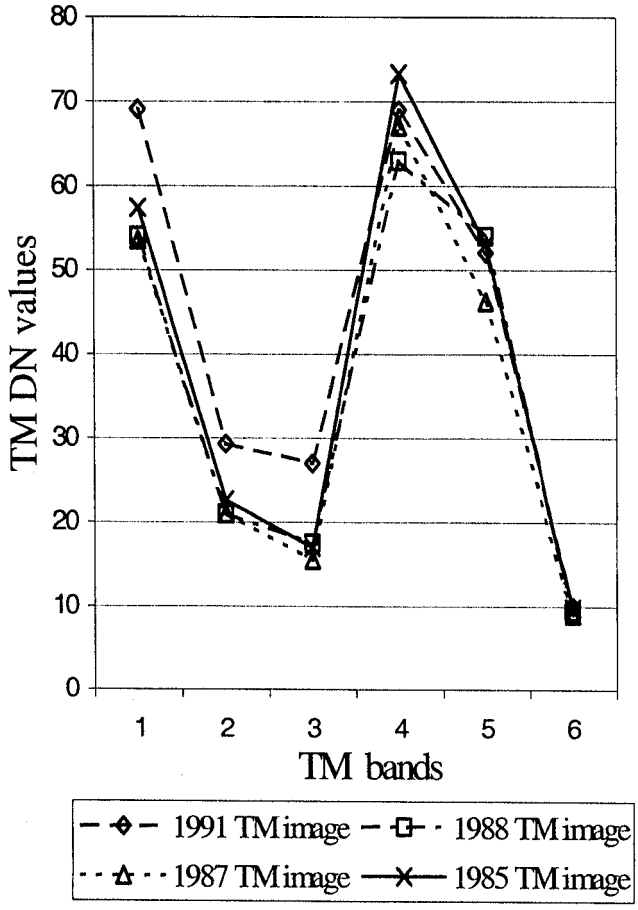

Figure 5. Comparison of raw TM data (forest).

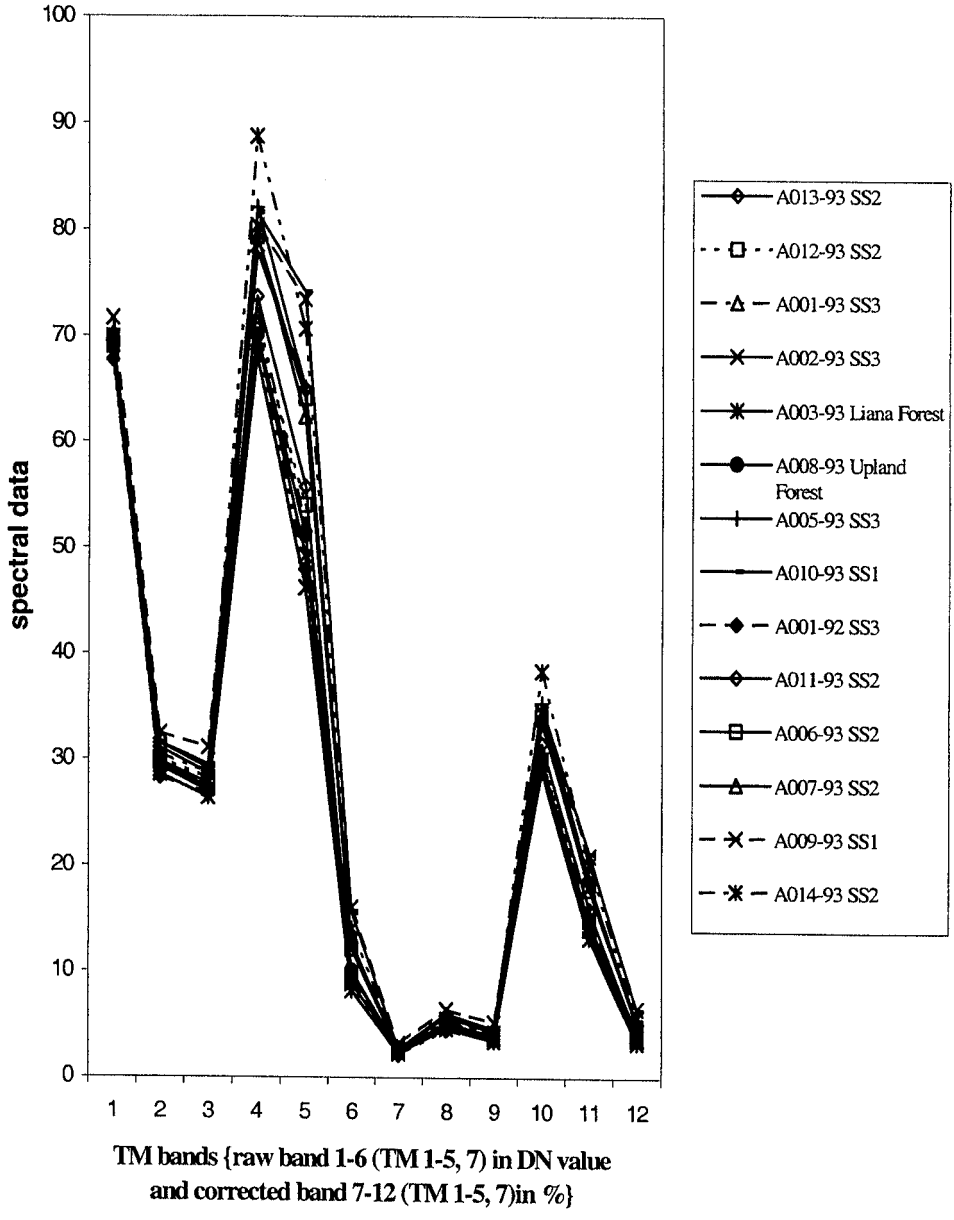

Figure 6. Comparison between raw data and corrected data (1991 TM Image).

8.2. *Statistical analysis of surface reflectance*

Table 4 lists the basic statistics: minimum, maximum, range, mean and standard deviation for each band from using different correction methods. The range and standard deviation from the apparent reflectance model and DOS model have the same values for each band, but the maximum, minimum and mean values are different. This indicates that the results produced from these two methods hold the same information loads and the same relative range of data distribution. For image appearance from single scenes, these two methods get the same results. The only difference

Table 4. Statistical values associated with different correction methods.

Bands	Methods	Minimum	Maximum	Range	Mean	Std. deviation
TM 1	DATE1	7.60	18.24	10.64	9.07	0.6327
	DATE2	0.65	11.29	10.64	2.13	0.6327
	GAIN1	6.22	14.92	8.70	7.43	0.5175
	GAIN2	0.54	9.23	8.69	1.74	0.5174
	COST1	0.93	16.12	15.19	3.04	0.9038
	COST2	0.76	13.19	12.43	2.48	0.7391
TM 2	DATE1	5.11	19.54	14.43	7.04	1.1894
	DATE2	1.97	16.39	14.42	3.89	1.1894
	GAIN1	4.37	16.68	12.31	6.01	1.0150
	GAIN2	1.68	13.99	12.31	3.32	1.0150
	COST1	2.52	21.02	18.50	4.99	1.5200
	COST2	2.15	17.94	15.79	4.26	1.3012
TM 3	DATE1	3.50	28.64	25.14	5.60	1.7885
	DATE2	1.51	26.65	25.14	3.61	1.7885
	GAIN1	2.60	21.38	18.78	4.17	1.3356
	GAIN2	1.13	19.91	18.78	2.70	1.3356
	COST1	1.78	31.36	29.58	4.25	2.1044
	COST2	1.33	23.42	22.09	3.17	1.5711
TM 4	DATE1	0.45	51.47	51.02	27.24	5.3895
	DATE2	0.39	51.41	51.02	27.10	5.3895
	GAIN1	0.39	45.00	44.61	23.82	4.7115
	GAIN2	0.34	44.95	44.61	23.77	4.7115
	COST1	0.43	56.50	56.07	29.87	5.9200
	COST2	0.37	49.39	49.02	26.12	5.1778
TM 5	DATE1	−0.92	58.10	59.02	15.72	5.1915
	DATE2	0	59.02	59.02	16.64	5.1915
	GAIN1	−0.73	45.92	46.65	12.42	4.1031
	GAIN2	0	46.65	46.65	13.15	4.1031
	COST1	0	59.02	59.02	16.64	5.1915
	COST2	0	46.65	46.65	13.15	4.1031
TM 7	DATE1	−0.96	39.75	40.71	3.82	2.5800
	DATE2	0	40.73	40.73	4.78	2.2800
	GAIN1	−0.87	35.85	36.72	3.44	2.3261
	GAIN2	0	36.72	36.72	4.31	2.3261
	COST1	0	40.73	40.73	4.78	2.5800
	COST2	0	36.72	36.72	4.31	2.3261

is the absolute reflectance values because the DOS model corrects for the path radiance that has the additive function for the reflectance. The reflectance in near and middle infrared bands have similar values due to the weak effects of atmospheric scattering on them. The apparent reflectance model has another disadvantage in that it overcorrects the reflectance, especially the dark objects, in middle infrared bands that make the minimum reflectance negative. Actually all the models based on the image measurement overcorrect the reflectance in the middle infrared wavelengths. This is because these models do not have the capability to simulate the atmospheric absorption that decreases the surface reflectance. The Improved Image-based DOS model, especially the COST1 produces the widest range of spectral data and has the largest information loads for each band. The data in this table indicate that whether the path radiance of the single scenes was removed or does not improve the information loads and image appearance because it only changes the absolute surface reflectance and does not change the relative values of the image. However, the removal

of path radiance is important not only for converting to surface reflectance, but also for temporal and spatial atmospheric correction so that the surface reflectance has the consistency and comparability among different dates of images or different scenes of images. This is due to the different path radiance with different atmospheric conditions. The removal of atmospheric transmittance can improve the image quality and information loads. This is because the atmospheric transmittance has multiplicative influences on the image and directly change the reflectance.

9. Conclusions

Many techniques have been developed for atmospheric correction. Physically-based models such as 6S and LOWTRAN7 are very complex and require the *in situ* atmospheric information at the same time of satellite overflight. This requirement greatly limits their applications, especially for the historical remotely sensed data due to the difficulty in collecting the atmospheric information. The relative calibration methods such as dark pixel subtraction and histogram matching are too coarse to be applied in many applications that require relatively high accuracy of surface reflectance. The image-based models such as apparent reflectance model, DOS model and Improved Image-based DOS model are simple and easy to apply. They are purely based on the image measurements and do not required *in situ* atmospheric information. The apparent reflectance model is not suitable for the correction when the application requires accurate surface reflectance because this model does not correct for the atmospheric scattering and absorption. The correction of the atmospheric scattering is very important, especially for the shorter visible wavelength bands because the path radiance has serious effects on them. An additional disadvantage of this model is that it overcorrects the surface reflectance, especially for the dark objects in the middle infrared bands. The DOS model corrects for the path radiance and produces higher accurate surface reflectance than that from the apparent reflectance model. Because the DOS model corrects for the effects of atmospheric scattering, it makes the surface reflectance comparable among multitemporal images, especially in the visible bands. However, the DOS model does not correct the atmospheric transmittance. The Improved Image-based DOS model takes the atmospheric scattering and absorption into account. It corrects the effects caused by path radiance and part of the atmospheric transmittance. This model can be used for the atmospheric correction for most of the remotely sensed data application, especially for the historical image data when atmospheric data are not available.

When atmospheric correction is used for the historical image data, it is appropriate to use the image acquisition date formula to convert the DN values to the at-satellite radiance if the gain and bias are not available in the image header file because the experimental maximal and minimal spectral radiance underestimate the radiance. In this article Improved Image-based DOS model combining the image acquisition date formula was found to be the best model for correcting the atmospheric effects in the Amazon basin in such a situation that atmospheric data, even the image header file information, are not available. However, attention should be paid to the identification of path radiance and the estimation of atmospheric transmittance. Comprehensive analysis of the image histogram, dark objects, and image statistics are necessary to find appropriate path radiance for each band separately. Further research should be focused on how to better identify the path radiance, how to estimate the atmospheric transmittance, and the accuracy analysis of the surface reflectance to further refine the Improved Image-based DOS model applications.

Acknowledgements

The authors wish to acknowledge the support of the National Science Foundation (95–21918 and 93–10049), the National Institutes of Health's NICHD (9710386A) and support from NASA's LBA program (through grant N005-334) that made the data collection and analysis for this paper possible. The authors also wish to acknowledge the assistance of many Brazilian collaborators (among them Italo Claudio Falesi, Adilson Serrao, Flavio Ponzoni, Dalton Valeriano and others at EMBRAPA-CPATU), Indiana State University collaborators (among them Ping Jiang and Hui Li) and a host of North American collaborators (among them Glen Green, J. C. Randolph, Joanna Tucker, Lindan Hill and Bruce Boucek). None of these colleagues or funding agencies should be held responsible for the views presented herein. They are the sole responsibility of the authors.

References

BRONDIZIO, E., MCCRACKEN, S., MORAN, E., SIQUEIRA, A., NELSON, D., and RODRIGUEZ-PEDRAZA, C., In press, The colonist footprint: towards a conceptual framework of deforestation trajectories among small farmers in frontier Amazonia. In *Patterns and Processes of Land use and Forest Change in the Amazon*, edited by C. Wood *et al.* (Gainesville: University of Florida Press).

CAMPBEL, G. S., and NORMAN, J. M., 1998, *An introduction to environmental biophysics*, 2nd edn (New York: Springer-Verlag Inc.).

CHAVEZ, P. S. JR, 1988, An improved dark-object subtraction technique for atmospheric scattering correction of multispectral data. *Remote Sensing of Environment*, **24**, 459–479.

CHAVEZ, P. S. JR, 1989, Radiometric calibration of Landsat Thematic Mapper multispectral images. *Photogrammetric Engineering and Remote Sensing*, **55**, 1285–1294.

CHAVEZ, P. S. JR, 1996, Image-based atmospheric corrections – revisited and improved. *Photogrammetric Engineering and Remote Sensing*, **62**, 1025–1036.

DUGUAY, C. R., and LEDREW, E. F., 1992, Estimating surface reflectance and albedo from Landsat-5 Thematic Mapper over rugged terrain. *Photogrammetric Engineering and Remote Sensing*, **58**, 551–558.

ERDAS INC., 1997, *ERDAS IMAGINE: ERDAS field guide*, 4th edn (Atlanta: ERDAS, Inc.)

FRASER, R. S., FERRAZE, R. A., KAUFMAN, Y. J., MARKHAM, B. L., and MATTOO, S., 1992, Algorithm for atmospheric correction of aircraft and satellite imagery. *International Journal of Remote Sensing*, **13**, 541–557.

GILABERT, M. A., CONESE, C., and MASELLI, F., 1994, An atmospheric correction method for the automatic retrieval of surface reflectance from TM images. *International Journal of Remote Sensing*, **15**, 2065–2086.

GRATTON, D. J., HOWARTH, P. J., and MARCEAU, D. J., 1993, Using Landsat-5 Thematic Mapper and digital elevation data to determine the net radiation field of a mountain glacier. *Remote Sensing of Environment*, **43**, 315–331.

HALL, D. K., CHANG, A. T. C., and SIDDALINGAIAH, H., 1988, Reflectance of glaciers as calculated using Landsat-5 Thematic Mapper data. *Remote Sensing of Environment*, **25**, 311–321.

HALL, D. K., CHANG, A. T. C., FOSTER, J. L., BENSON, C. S., and KOVALICK, W. M., 1989, Comparison of in situ and Landsat derived reflectance of Alaskan glaciers. *Remote Sensing of Environment*, **28**, 23–31.

HALL, F. G., STREBEL, D. E., NICKSON, J. E., and GEOTZ, S. J., 1991, Radiometric rectification toward a common radiometric response among multidate, multisensor images. *Remote Sensing of Environment*, **35**, 11–27.

HILL, J., 1991, A quantitative approach to remote sensing: sensor calibration and comparison. In *Remote Sensing and Geographical Information Systems for Resource Management in Developing Countries*, edited by A. S. Belward and C. R. Valenzuela (Boston, Mass.: Kluwer Academic Publishers), pp. 97–110.

HILL, J., and BORIS, S., 1991, Radiometric correction of multi-temporal Thematic Mapper data for use in agricultural land-cover classification and vegetation monitoring. *International Journal of Remote Sensing*, **12**, 1471–1491.

ITTEN, K. I., MEYER, P., KELLENBERGER, T., LEU, R., SANDMEIER, S. T., BITTER, P., and SEIDEL, K., 1992, Correction of the impact of topography and atmosphere on Landsat TM forest mapping of Alpine regions. *Remote Sensing Series*, vol. 18, University of Zurich, 50 pp.

ITTEN, K. I., and MEYER, P., 1993, Geometric and radiometric correction of TM-data of mountainous forested areas. *IEEE Transactions on Geoscience and Remote Sensing*, **31**, 764–770.

JENSEN, J. R., 1996, *Introduction digital image processing: A remote sensing perspective*, 2nd edn (New York: Prentice Hall).

KAWATA, Y., VENO, S., and KUSAKA, T., 1988, Radiometric correction for atmospheric and topographic effects on Landsat MSS images. *International Journal of Remote Sensing*, **9**, 729–748.

KAUFMAN, Y. J., and SENDRA, C., 1988, Algorithm for automatic atmospheric correction to visible and near-IR satellite imagery. *International Journal of Remote Sensing*, **9**, 1357–1381.

KUSAJA, K., and KAWATA, Y., 1994, Atmospheric and topographic correction of satellite data over mountainous terrain. In *Proceedings of the 1994 International Geoscience and Remote Sensing Symposium (IGARSS '94), 8–12 August 1994, California Institute of Technology, Pasadena, California* (Spring, Tex.: IEEE GRSS), pp. 14–29.

LEPRIEUR, C. E., DURAND, J. M., and PEYRON, J. L., 1988, Influence of topography on forest reflectance using Landsat Thematic Mapper and digital terrain data. *Photogrammetric Engineering and Remote Sensing*, **54**, 491–496.

LEPRIEUR, C., CARRERE, V., and GU, X. F., 1995, Atmospheric correction and ground reflectance recovery for airborne visible/infrared imaging spectrometer (AVIRIS) data: MAC Europe' 91. *Photogrammetric Engineering and Remote Sensing*, **61**, 1233–1238.

MARKHAM, B. L., and BARKER, J. L., 1985, Spectral characterization of the LANDSAT Thematic Mapper sensors. *International Journal of Remote Sensing*, **6**, 697–716.

MARKHAM, B. L., and BARKER, J. L., 1986, Landsat MSS and TM post-calibration dynamic ranges, exoatmospheric reflectance and at-satellite temperatures. *EOSATLandsat Technical Notes*, **1**, 3–8.

MARKHAM, B. L., and BARKER, J. L., 1987, Thematic Mapper bandpass solar exoatmospheric irradiances. *International Journal of Remote Sensing*, **8**, 517–523.

MAUSEL, P., WU, Y., LI, Y., MORAN, E. F., and BRONDIZIO, E. S., 1993, Spectral identification of successional stages following deforestation in the Amazon. *Geocarto International*, **8**, 61–81.

MEYER, P., ITTEN, K. I., KELLENBERGER, J., SANDMEIER, S., and SAMMEIER, R., 1993, Radiometric correction of topographically induced effects on Landsat TM data in an alpine environment. *ISPRS Journal of Photogrammetry and Remote Sensing*, **48**, 17–28.

MILTON, E. J., 1994, Teaching atmospheric correction using a spreadsheet. *Photogrammetric Engineering and Remote Sensing*, **60**, 751–754.

MORAN, E. F., 1981, *Developing the Amazon* (Bloomington: Indiana University Press).

MORAN, M. S., JACKSON, D., SLATE, P. N., and TEILLET, P. M., 1992, Evaluation of simplified procedures for retrieval of land surface reflectance factors from satellite sensor output. *Remote Sensing of Environment*, **41**, 169–184.

MORAN, E. F., BRONDIZIO, E. S., and MAUSEL, P., 1994, Secondary succession. *National Geographic Research and Exploration*, **10**, 458–476.

MORAN, E. F., BRONDIZIO, E. S., MAUSEL, P., and WU, Y., 1994, Integrating Amazonian vegetation, land use, and satellite data. *BioScience*, **44**, 329–338.

MULLER, E., 1993, Evaluation and correction of angular anisotropic effects in multidate SPOT and Thematic Mapper data. *Remote Sensing of Environment*, **45**, 295–309.

OLSSON, H., 1993, Regression function for multitemporal relative calibration of Thematic Mapper data over boreal forest. *Remote Sensing of Environment*, **46**, 89–102.

OLSSON, H., 1995, Reflectance calibration of Thematic Mapper data for forest change detection. *International Journal of Remote Sensing*, **16**, 81–96.

PRICE, J. C., 1987, Calibration of satellite radiometers and the comparison of vegetation indices. *Remote Sensing of Environment*, **21**, 15–27.

PALLUCONI, F., HOOVER, C., ALLEY, R., JENTOFT-NILSEN, M., and THOMPSON, T., 1996, An atmospheric correction method for ASTER thermal radiometry over land. ASTER Standard Data Product, AST09.

PROY, C., TANRE, D., and DESCHAMPS, P. Y., 1989, Evaluation of topographic effects in remotely sensed data. *Remote Sensing of Environment*, **30**, 21–32.

PUTSAY, M., 1992, A simple atmospheric correction method for the short wave satellite images. *International Journal of Remote Sensing*, **13**, 1549–1558.

RAHMAN, H., and DEDIEU, G., 1994, SMAC: A simplified method for the atmospheric correction of satellite measurements in the solar spectrum. *International Journal of Remote Sensing*, **15**, 123–143.

RICHARDS, J. A., 1993, *Remote sensing digital image processing: An introduction*, 2nd edn (New York: Springer-Verlag).

RICHTER, R., 1985, Some aspects of the atmospheric radiance model of LOWTRAN6. *International Journal of Remote Sensing*, **6**, 1773–1777.

RICHTER, R., 1996a, A spatially adaptive fast atmospheric correction algorithm. *International Journal of Remote Sensing*, **17**, 1201–1214.

RICHTER, R., 1996b, Atmospheric correction of DAIS hyperspectral image data. *Computers and Geosciences*, **22**, 785–793.

RICHTER, R., 1997, Correction of atmospheric and topographic effects for high spatial resolution satellite imagery. *International Journal of Remote Sensing*, **18**, 1099–1111.

ROBINOVE, C. J., 1982, Computation with physical values from Landsat digital data. *Photogrammetric Engineering and Remote Sensing*, **48**, 781–784.

SCHOTT, J. R., SALVAGGIO, C., and VOLCHOK, W. J., 1988, Radiometric scene normalization using pseudoinvariant features, *Remote Sensing of Environment*, **26**, 1–26.

SLATE, P. N., 1980, *Remote sensing optics and optical systems* (White Plains, NY: Addison-Wesley).

STEFAN, S., and ITTEN, K. I., 1997, A physically-based model to correct atmospheric and illumination effects in optical satellite data of rugged terrain. *IEEE Transactions on Geoscience and Remote Sensing*, **35**, 708–717.

TANRE, D., DEROO, C., DUHAUT, P., HERMAN, M., MORCREOTE, J. J., PERBOS, J., and DESCHOMPS, P. Y., 1990, Technical note: description of a computer code to simulate the satellite signal in the solar spectrum: the 5S code. *International Journal of Remote Sensing*, **11**, 659–668.

TEILLET, P. M., 1986, Image correction for radiometric effects in remote sensing. *International Journal of Remote Sensing*, **7**, 1637–1651.

TEILLET, P. M., and FEDOSEJEVS, G., 1995, On the dark target approach to atmospheric correction of remotely sensed data. *Canadian Journal of Remote Sensing*, **21**, 374–387.

TEILLET, P. M., GUINDON, B., and GOODENOUGH, D. G., 1982, On the slope-aspect correction of multispectral scanner data. *Canadian Journal of Remote Sensing*, **8**, 84–106.

THOME, K., MARKHAM, B., BARKER, J., SLATER, P., and BIGGAR, S., 1997, Radiometric calibration of Landsat. *Photogrammetric Engineering and Remote Sensing*, **63**, 835–858.

THOME, K. J., BIGGAR, S. F., GELLMAN, D. I., and SLATE, P. N., 1994, Absolute radiometric calibration of Landsat-5 Thematic Mapper and spaceborne thermal emission and reflection radiometer. In *Proceedings of the 1994 International Geoscience and Remote Sensing Symposium (IGARSS '94), 8–12 August 1994, California Institute of Technology, Pasadena, California (Spring, Tex.: IEEE GRSS).*

VERMOTE, E., TANRE, D., DENZE, J. L., HERMAN, M., and MORCRETTE, J. J., 1994, Second simulation of the satellite signal in the solar spectrum (6S). User guide version 2.

VERMOTE, E., TANRE, D., DEUZE, J. L., HERMAN, M., and MORCRETTE, J. J., 1997, Second simulation of the satellite signal in the solar spectrum, 6S: An overview. *IEEE Transactions on Geoscience and Remote Sensing*, **35**, 675–686.

VOLCHOK, W. J., and SCHOTT, J. R., 1986, Scene to scene radiometric normalization of the reflected bands of the Landsat Thematic Mapper. In *Proceedings of the SPIE Symposium, Earth Remote Sensing Using the Landsat Thematic Mapper and SPOT Sensor Systems, April 1985, Innsbruck, Austria*, vol. 660, edited by P. N. Slater (Bellingham, Wash.: The International Society for Optical Engineering), pp. 9–17.